Int. J. Electrochem. Sci., 11 **(2016)** 5792 – 5799, doi: 10.20964/2016.07.55

International Journal of
ELECTROCHEMICAL
SCIENCE
www.electrochemsci.org

Short Communication

Preparation of $Li_4Mn_5O_{12}$-Li_2MnO_3 1D Nanocomposite as Cathode for Lithium Ion Batteries

Guanrao Liu, Shichao Zhang[*]*, Shengbin Wang*

School of Materials Science &Engineering, Beijing University of Aeronautics & Astronautics, Beijing 100191, China
[*]E-mail: csc@buaa.edu.cn

Received: 17 April 2016 / *Accepted:* 22 May 2016 / *Published:* 4 June 2016

The $Li_4Mn_5O_{12}$-Li_2MnO_3 1D nanocomposite with 200~400nm diameter and 3~5μm length have been synthesized by MnOOH nanorods and $LiOH{\cdot}H_2O$ via a solid state reaction process. The electrochemical properties and the mechanism were studied by the galvanostatic charging/discharging test and cyclic voltammograms (CV) test. The initial discharge capacity values were 111 $mAh{\cdot}g^{-1}$ at 0.5C rate and 88 $mAh{\cdot}g^{-1}$ at 1C rate observed in the range of 3.3–2.3V. Benefit from the one-dimension structure, high crystallinity and the existence of Li_2MnO_3 layer, the $Li_4Mn_5O_{12}$-Li_2MnO_3 electrode exhibits excellent rate capability and cycling stability, with 92% and 99% capacity retention after 100 cycles at 0.5C and1C rate, respectively.

Keywords: $Li_4Mn_5O_{12}$, Cathode materials, Electrochemical performance, Lithium-ion battery, 1D nanostructures

1. INTRODUCTION

Nanoscaled electrode materials have been researched widely to enhance the electrochemical performance of lithium-ion batteries (LIBs), essentially because of their substantial advantages in terms of Li^+ ion transport. In the nanostructure, the Li^+ intercalation/deintercalation strain can decreases with the reduction of Li-diffusion length, leading to the better cycle life. In addition, nanosized electrode materials owing to their large specific surface area can provide a large electrode/electrolyte contact area for Li^+ diffusing into structure [1-4]. It is well known that the component structure can significantly improve the performance of electrode materials, because the electrochemical properties of materials are strongly influenced by their composition, structure, morphology, and homogeneity. Among these nano-sized electrode materials, one-dimensional (1D) nanostructures such as nanowires and nanorods, bring the dimensions in the two directions

perpendicular to long axis of the particles comparable to the mean-free-path length of electrons[5], i.e. they can offer efficient one-dimensional electron transport pathways, and make facile strain relaxation during battery charging/discharging.

Because of the advantages of outstanding cyclic stability, high coulombic efficiency, and the excellent structural stability, spinel lithium manganese oxides with 3D interstitial space for Li^+ cation transportation as an electrode material for 3V rechargeable lithium batteries, is one of the most important Li-Mn-O materials [6, 7]. Among these, extensive efforts have been devoted to spinel $LiMn_2O_4$ for its high capacity[8, 9], but one of the major defects is to suffer from poor cycling stability, due to the Jahn-Teller distortion when the average oxidation state of Mn falls below 3.5+[10,11]. However, $Li_4Mn_5O_{12}$ component with a theoretical capacities of 163 $mAh \cdot g^{-1}$ possess a layered-spinel hybrid structure, in which oxidation state of Mn is +4, thus the Jahn-Teller distortion can be suppressed, and the cycling stability of the materials is enhanced while the higher degree of lithium intercalation into the 16c sites occurs [12-14]. It has been demonstrated that $Li_4Mn_5O_{12}$ nanowires exhibit an excellent electrochemistry performance as cathode materials for LIBs [15]. It was reported that $Li_4Mn_5O_{12}$-Li_2MnO_3 structure delivered a good electrochemical performance in the 3V-range, because Li_2MnO_3 shell exhibits merit of structural compatibility with the spinel and being Li^+ conductor which is propitious to the capacity retention [16]. In this work, we demonstrate a facile route to synthesize $Li_4Mn_5O_{12}$-Li_2MnO_3 1D nanostructures by solid-state reaction using MnOOH nanorods as self-template, and Li^+ storage properties were investigated. The resulting 1D structure consists of amounts of well-crystallized nanorods with diameters of 200nm. The electrochemical tests manifest that the obtained cathode materials have a high capacity retention which is 92% at 1/2C rate, 99% at 1C rate respectively after 100 cycles because of the stable composite structure.

2. EXPERIMENTAL

2.1. Preparation and characterization of $Li_4Mn_5O_{12}$-Li_2MnO_3 nanorods

There are two steps for obtaining $Li_4Mn_5O_{12}$-Li_2MnO_3 nanorods:

2.1.1. Synthesis of the precursor MnOOH nanorods

MnOOH nanorods were synthesized from the mixed aqueous solution with reactants and surfactant cetyltrimethyl ammonium bromide (CTAB) by hydrothermal reaction [17, 18]. In typical procedure, CTAB, $KMnO_4$ and $MnSO_4$ were dissolved in distilled water ($KMnO_4$:$MnSO_4$=1: 4, molar ratio). And then, excess LiOH solution was added into the mixed solution. A brown suspension was immediately formed as soon as LiOH solution was added. The mixed solution was then transferred into a Teflon-lined stainless steel autoclave for a hydrothermal process at 200℃ for 32 h. Finally, the obtained precipitate washed thoroughly with distilled water and ethanol, and dried at 60℃ in air.

2.1.2. Preparation of $Li_4Mn_5O_{12}$- Li_2MnO_3 nanorods

The $Li_4Mn_5O_{12}$- Li_2MnO_3 nanorods was prepared via a simple solid-state reaction: as-prepared MnOOH nanorods and $LiOH·H_2O$ with a molar ratio 1:1 were dispersed into ethanol, grounded to be well-mixed, and dried at 60℃ in air. Finally, the mixtures were calcined at 650℃ for 15h, and then kept at 800℃ for 12h.

2.2. Structure Characterization

X-ray powder diffraction (XRD) measurements were employed to investigate the crystallographic structure using a Rigaku Rint2200 X-ray diffractormeter with a non-monochromated Cu-Kα X-ray source. The morphology and structure of prepared materials were exhibited by transmission electron microscopy (TEM) images recorded with a JEOL-2100F instrument at an acceleration voltage of 200 kV， and scanning electron microscopy (SEM) images recorded by a HITACHI S4800.

2.3. Electrochemical measurements

Electrochemical properties of the prepared samples were measured using Swagelok-type two-electrode cells. The working electrodes were pressed with a mixture of 80 wt.% active materials, 15 wt.% acetylene black, and 10 wt.% polytetrafluoroethylene (PTFE) binders. Then, the prepared electrodes were dehydrated by a vacuum dry at 60℃for 12 h and were cooled down to room temperature. The cells assembled in an MBraun glove box filled with pure argon gas. A lithium disk served as counter and reference electrodes. The electrolyte was 1M $LiPF_6$ dissolved in ethylene carbonate (EC) and dimethyl carbonate (DMC) with a volume ratio of 1:1. Celgard 2300 polypropylene was employed as the separator. The galvanostatical charging/discharging measurement was performed by the battery test system-NEWARE BTS-610 (Neware Technology Co., Ltd., China) with a cut-off voltage of 2.3V-3.3V (versus Li/Li^+) at ambient temperature. The current density were according to $Li_4Mn_5O_{12}$ with the specific capacity 160mAh·g-1. The Cyclic Voltammograms (CV) test was recorded between 2.2 V and 3.4 V versus Li/Li^+ at a scan rate $0.1mV·s^{-1}$ using CHI 1100 instrument.

3. RESULT AND DISCUSSION

3.1. Structures and Morphologies Analysis

The structure and morphology of the precursor were characterized by XRD and SEM. As shown in Fig.1a, all peaks of the pattern can be indexed to monoclinic structured γ-MnOOH (JCPDS No. 41-1379). The synthesis of MnOOH can be described as [17, 18]:

$$2KMnO_4+8MnSO_4+12H_2O \rightarrow 10MnOOH+K_2SO_4+7H_2SO_4 \quad (1)$$

The morphology of MnOOH was nanorods with a diameter of 200~400nm and a length of 10μm (Fig.1b), indicating it can be used as precursor and template for preparing 1D lithium manganese oxide.

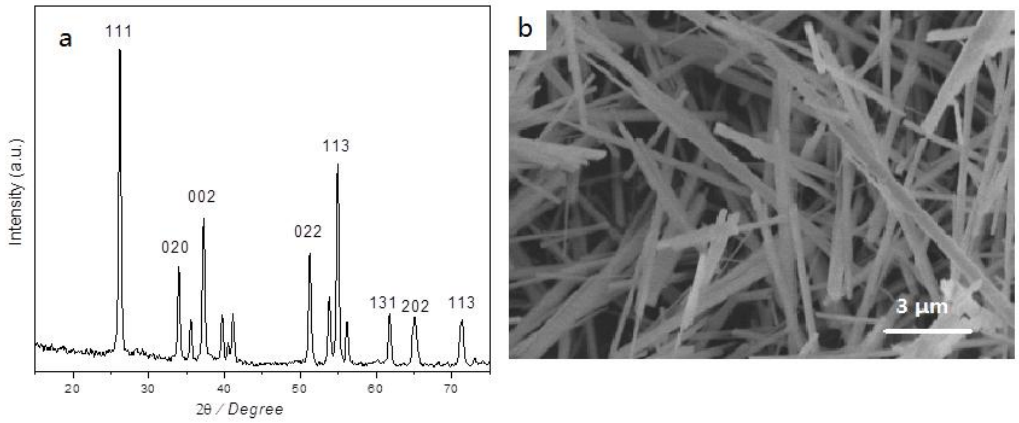

Figure 1. a) XRD patterns and b)SEM images of the prepared precursor MnOOH

The following solid state reaction for the formation of $Li_4Mn_5O_{12}$ was divided into two steps: MnO_2 firstly formed at 280℃ [19], then $Li_4Mn_5O_{12}$ nanorods were obtained at 650℃, the chemical equations are as follows:

$$4MnOOH+O_2 \rightarrow 4MnO_2 + 2H_2O \quad (2)$$

$$5MnO_2 +4LiOH \rightarrow Li_4Mn_5O_{12} + 2H_2O \quad (3)$$

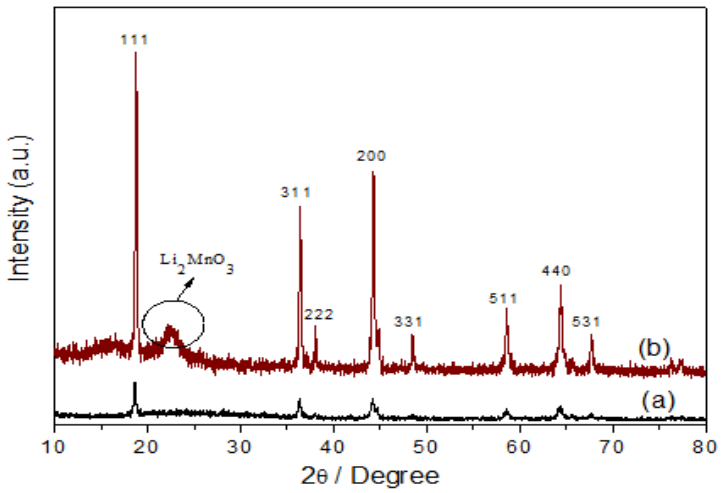

Figure 2. XRD patterns of $Li_4Mn_5O_{12}$ and $Li_4Mn_5O_{12}$-Li_2MnO_3 composite.

Fig.2 present the XRD patterns of the samples prepared at 650℃ (a) and samples with further heat-treatment at 800℃ (b) respectively. All the peaks of sample (a) were identical to the index of $Li_4Mn_5O_{12}$ (JCPDS, No. 46-0810), but its crystallinity was not good enough. After the heat-treatment

at 800℃ (sample b), a small peak appeared at 20-25°corresponding to (020) and (110) planes monoclinic Li_2MnO_3 phase with space group of *C2/m*, resulting from a phase transformation from lithium-rich spinel containing Mn^{3+} ($Li_{1+x}Mn_{2-x}O_4$ with x<0.33) to Li_2MnO_3 (all Mn^{4+})[20-22]. Obviously, the standard peaks of these two phases are similar to each other and the locations of some peaks are very closer, indicating an easy transformation of structure between them [22]. In addition, the diffraction peaks of sample-b are quite narrow and sharp, demonstrating a high crystallinity of the prepared cathode materials.

Fig. 3a and 3b illustrated the morphology of sample-a and sample-b, both of them are nanorods with a diameter of 200~400nm and the length of 3~5μm, indicating that the product inherited the one-dimension morphology of MnOOH nanorods during the process, except a little fracture in length because of the high temperature. The detailed information of integrated layered-spinel structures of sample-b were evidenced by TEM and HRTEM (Fig.3c and 3d). There are two phases of layered and spinel structures existing in sample-b, i.e. layered monoclinic structure Li_2MnO_3 with the (020) planes, and the spinel $Li_4Mn_5O_{12}$ phase with the (111) planes [12]. The distribution of the layered-spinel hybrid structure in sample-b can be easily recognized.

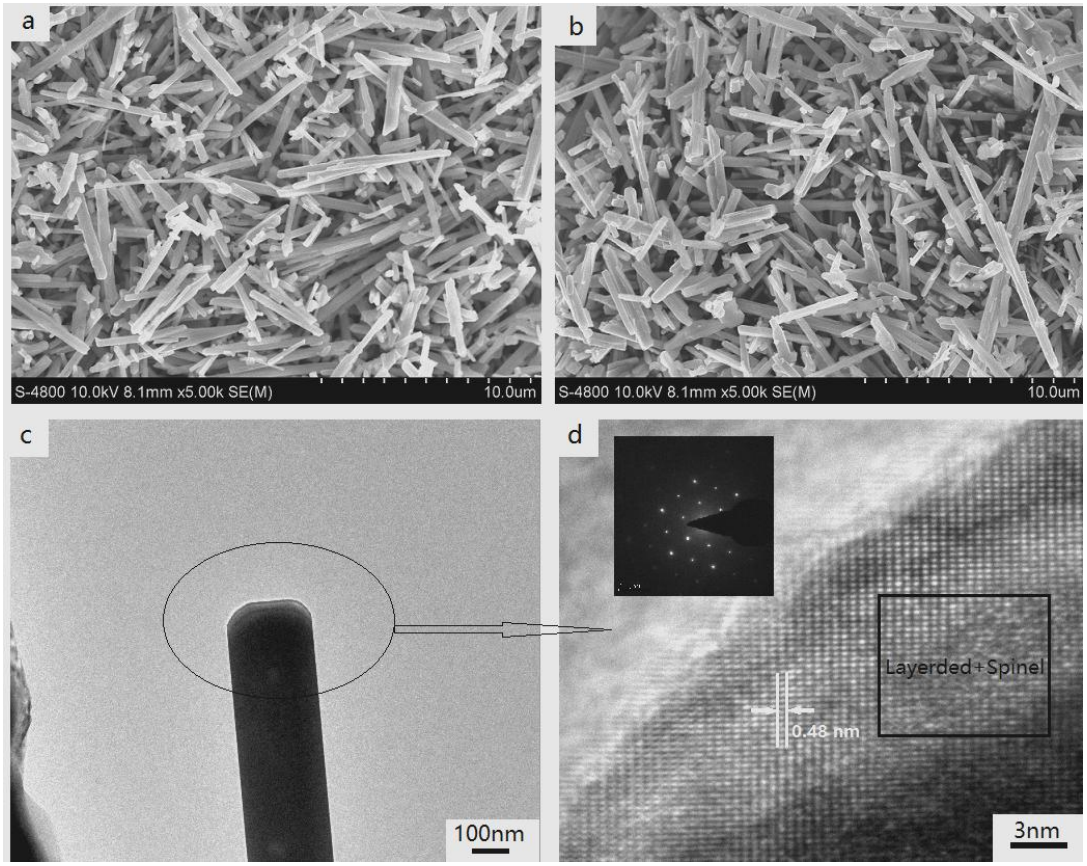

Figure 3. SEM images of (a) sample-a, (b) sample-b, (c) TEM and (d) HRTEM images of sample-b.

Combined with the XRD results, $Li_4Mn_5O_{12}$ is a lithium-poor phase compared with the lithium-rich layered phase, thus the Li^+ ions heterogeneously distributed in $Li_4Mn_5O_{12}$ will transfer into

Li_2MnO_3 phase during higher treatment temperature. The hybrid structure was successfully prepared by addition heat treatment process. Moreover, the crystallinity of $Li_4Mn_5O_{12}$ was improved during this process.

3.2. Electrochemical Properties

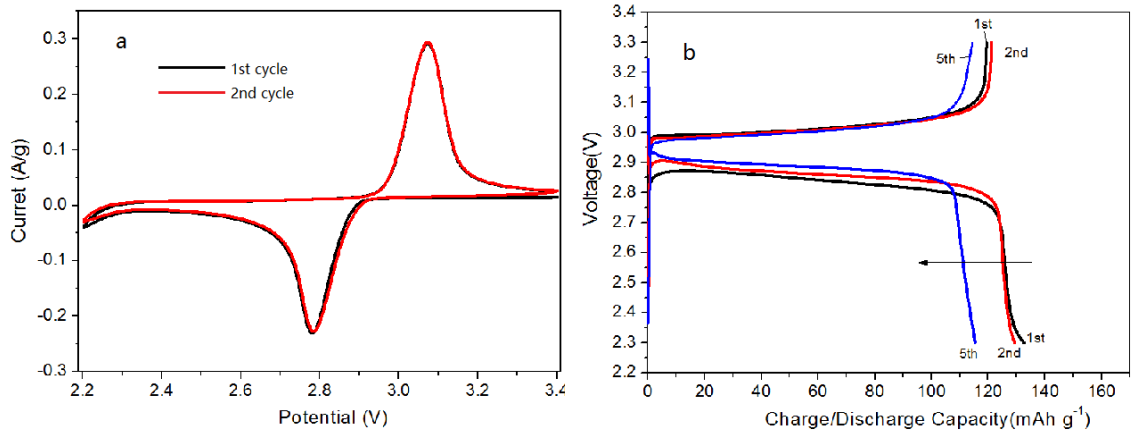

Figure 4. a) CV plots at 0.1 mVs^{-1} of $Li_4Mn_5O_{12}$- Li_2MnO_3 in the range of 3.3–2.3V and (b) the charge/discharge curves at 0.2C

The electrochemical performance of the prepared 1D $Li_4Mn_5O_{12}$-Li_2MnO_3 nanorods as cathode materials for LIBs was evaluated. The cyclic voltammograms (CV) profiles for the first two cycles at a scan rate of 0.1 mV s^{-1} in the voltage range 3.3-2.3 V (vs. Li/Li^+) are shown in Fig.4a. A couple of reversible redox peaks can be seen at around the potentials of 2.80V (delithiation process) and 3.07V (lithiation process), which was consistent with $Li_4Mn_5O_{12}$ cathode materials [23, 24].

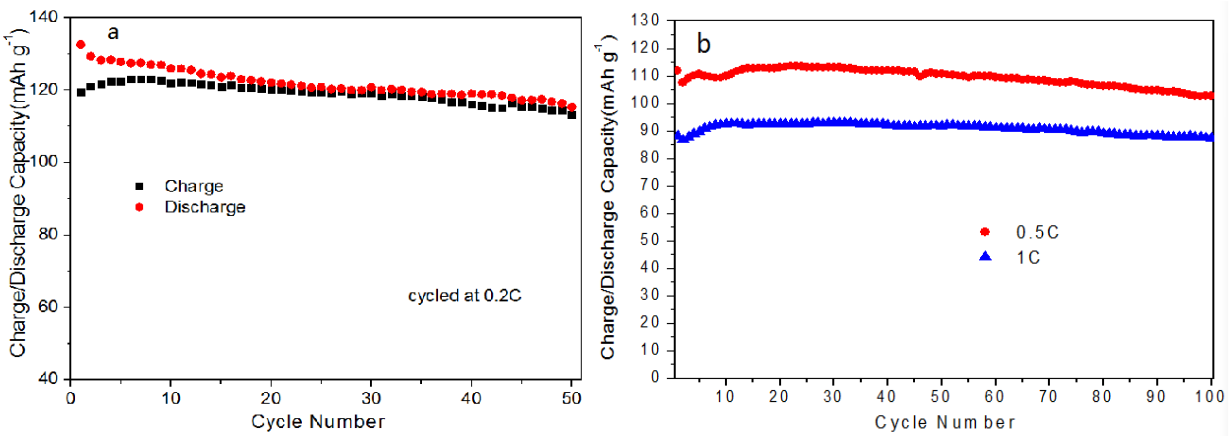

Figure 5. a) long-term cycling performance of the as-prepared $Li_4Mn_5O_{12}$- Li_2MnO_3 in the range of 3.3–2.3V, a) 0.2C (b) 0.5C and 1C

It was also found that the curves and redox peaks of second cycle basically overlapped with the

first cycle, indicating an outstanding reversibility in the electrochemical process. Fig.4b shows the first five charge/discharge curves of the $Li_4Mn_5O_{12}$-Li_2MnO_3 cathodes at 0.2C (as a theoretical storage capacity of 163 $mAh \cdot g^{-1}$) in a potential window of 3.3-2.3V at room temperature. The voltage profiles present two obvious long plateaus at 3.02 and 2.83 V respectively, exhibiting the typical characteristics of $Li_4Mn_5O_{12}$, which almost corresponded to the redox peaks of CV curves shown in Fig.4a. The initial charge/discharge capacity values were 119 $mAh \cdot g^{-1}$ and 132 $mAh \cdot g^{-1}$ respectively. The capacity tended to be stable after 5cycles.

To further evaluate the rate performance of the 1D $Li_4Mn_5O_{12}$-Li_2MnO_3 nanorods, the cathodes materials were cycled within a potential window of 3.3–2.3V, at 0.2C, 0.5C and 1C, respectively. As shown in Fig.5a, The initial charge capacity at 0.2C is lower than some previous report [25-27], but the capacity retention was 92% after 30 cycles. The initial discharge capacity values at 0.5C and 1C were 111 $mAh \cdot g^{-1}$ and 88 $mAh \cdot g^{-1}$ with the capacity retention of 92% and 99% after 100 cycles, respectively (Fig.5b). The capacity retention at 0.5C rate was lower than the one at 1C rate, owing to the longer test period of time, which was almost twice over the 1C rate. The longer test period could lead to the more volatilization of electrolyte, resulting in the more capacity grade. According to all the electrochemical tests above, the $Li_4Mn_5O_{12}$-Li_2MnO_3 nanorods appears an excellent rate performance, especially in high rate value, due to its 1D composite nanostructures with the advantages of large specific surface area and the reduction of Li-diffusion length.

4. CONCLUSIONS

In conclusion, $Li_4Mn_5O_{12}$–Li_2MnO_3 nanorods have been prepared with a facile, low-cost, and replicable solid-state routine. The products inherited the one-dimension morphology of the as-prepared MnOOH precursor. The electrochemical tests exhibit that the cathode materials with a discharge capacity of 132 $mAh \cdot g^{-1}$ at 0.2C and 111 $mAh \cdot g^{-1}$ at 0.5C rate, delivered an excellent cycle performance. The capacity retention of the products was 99% after 100 cycles at 1C, due to the nanoscale effect and the Li_2MnO_3 layer which makes it easier for Li^+ diffusion. The simple synthesis methods and the excellent electrochemical performances of 1D $Li_4Mn_5O_{12}$–Li_2MnO_3 composite nanostructures indicated their promising future for application as cathode materials in lithium-ion batteries.

ACKNOWLEDGEMENT
This work was supported by the National Basic Research Program of China (973 Program) (2013CB934001), National Natural Science Foundation of China (51274017), National 863 Program of China (2013AA050904), International S&T Cooperation Program of China (2012DFR60530).

References

1. Y. Zhao, Q.Y. Lai, Y. J. Hao, H. M. Zeng, H. Y. Chu, and Z. E. Lin, *J. Power Sources*, 195 (2010) 4400.
2. D. L. Ye, G. Zeng, K. Nogita, K. Ozawa, M. Hankel, D. J. Searles, L. and Z. Wang, *Adv. Funct. Mater.* 25 (2015) 7488.

3. Z. L. Xu, J. B. Wang, K. Zhang, H. Zheng, Z. X. Dai, J. N. Gui, and X. Q. Yang, *ACS Appl. Mater. Inter*. 6 (2014) 1219.
4. D. A. Tompsett, S. C. Parker, and M. S. Islam, *J. Am. Chem. Soc*. 136 (2014) 1418.
5. Z. L. Wang, Y. Liu, and Z. Zhang, Handbook of Nanophase and Nanostructured Materials, Kluwer Academic/Plenum Publishers, New York (2012).
6. Y. Shin, and A. Manthiram, *J. Electrochem. Soc.* 151 (2004) A204.
7. C. Liu, Z. Wang, C. Shi, E. Liu, C. He, N. Zhao, *ACS Appl Mater Inter*, 6 (2014) 8363.
8. K. Du, G. R. Hu, Z. D. Peng, and L. Qi, *Electrochim. Acta*, 55(2010) 1733.
9. Y. G. Wang, and Y. Y. Xia, *Electrochem. Commun.* 7 (2005) 1138.
10. G. G. Amatucci, A. Blyr, C. Sigala, A. S. Gozdz, D. Larcher, and J. M. Tarascon, *J. Power Sources*, 69 (1997) 11.
11. F. Wu, N. Li, Y. Su, L. Zhang, L. Bao, J. Wang, L. Chen, Y. Zeng, L. Dai, J. Peng, and S. Chen, *Nano. Lett.* 14(2014) 3550.
12. T. Takada, H. Hayakawa, E. Akiba, F. Izumi, and B.C. Chakoumakos, *J. Power Sources*, 68(1997) 613.
13. Y. C. Zhang, H. Wang, B. Wang, H. Yan, A. Ahniyaz, and M. Yoshimura, *Mater. Res. Bull.* 37(2002) 1411
14. C. M. Julien, and K. Zaghib, *Electrochim. Acta*, 50(2004)411.
15. P. G. Bruce, A. R. Armstrong, and R. Gitzendanner, *J. Mater. Chem.* 9 (1999) 193.
16. Y. Li, Y. Makita, Z. Lin, S. Lin, N. Nagaoka, and X. Yang, *Sol. Stat. Ionics*, 196 (2011) 34.
17. X. Wang, and Y. D. Li, *Chem. Eur. J.* 9 (2003) 300.
18. S. F. Hou, G. Rao Liu, and T. H Ji, *Rare Met. Mater. Eng.* 36 (2007) 160
19. Y. C. Zhang, T. Qiao, Y. H. Xiao, and W. D. Zhou, *J. Cryst. Growth*, 280 (2005) 652.
20. Y. Li, Y. Makita, Z. Lin, S. Lin, N. Nagaoka, and X. Yang, *Sol. Stat. Ionics*, 196 (2011)34.
21. S. H. Park, S. H. Kang, C. S. Johnson, K. Amine, and M. M. Thackeray, *Electrochem. Commun.* 9 (2007) 262,
22. D. Wang, X. Y Wang, R. Z. Yu, Y. S. Bai, G. Wang, M. H. Liu, and X. K. Yang, *Electrochim. Acta*, 190 (2016) 1142.
23. J. Kim, and A. Manthiram, *J. Electrochem. Soc.* 145 (1998) L53.
24. Y. Tian, D. R. Chen, X. L. Jiao, and Y. Z. Duan, *Chem. Commun.* 20(2007) 2072.
25. J. Y. Cao, J. Xie, G. S. Cao, T. J. Zhu, X. B. Zhao, and S. C. Zhang, *Electrochim. Acta*, 111(2013) 447.
26. Y. Fu, H. Jiang, Y. J. Hu, L. Zhang, and C. Z. Li, *J. Power Sources*,261 (2014) 306.
27. Z. Q. Xie, S. Ellis, W. W. Xu, D. Dye, J. Q. Zhao, and Y. Wang, *Chem. Commun.* 51(2015)15000.